Microbiota regulate intestinal epithelial gene expression by suppressing the transcription factor Hepatocyte nuclear factor 4 alpha

James M Davison, Colin R Lickwar, Lingyun Song, et al.

Genome Res. published online April 6, 2017
Access the most recent version at doi:10.1101/gr.220111.116

Microbiota regulate intestinal epithelial gene expression by suppressing the transcription factor Hepatocyte nuclear factor 4 alpha

James M. Davison[1,2], Colin R. Lickwar[1], Lingyun Song[3], Ghislain Breton[4], Gregory E. Crawford[3] and John F. Rawls[1,‡]

[1]Department of Molecular Genetics and Microbiology, Center for the Genomics of Microbial Systems, Duke University, Durham, North Carolina 27710, USA; [2]Department of Cell Biology and Physiology, University of North Carolina, Chapel Hill, North Carolina 27599, USA; [3]Department of Pediatrics, Division of Medical Genetics, Center for Genomic and Computational Biology, Duke University, Durham, North Carolina 27708, USA; [4]Department of Integrative Biology and Pharmacology, McGovern Medical School, Houston, Texas 77030, USA; ‡Corresponding Author.

ABSTRACT

Microbiota influence diverse aspects of intestinal physiology and disease in part by controlling tissue-specific transcription of host genes. However, host genomic mechanisms mediating microbial control of intestinal gene expression are poorly understood. Hepatocyte nuclear factor 4 (HNF4) is the most ancient family of nuclear receptor transcription factors with important roles in human metabolic and inflammatory bowel diseases, but a role in host response to microbes is unknown. Using an unbiased screening strategy, we found that zebrafish Hnf4a specifically binds and activates a microbiota-suppressed intestinal epithelial transcriptional enhancer. Genetic analysis revealed that zebrafish *hnf4a* activates nearly half of the genes that are suppressed by microbiota, suggesting microbiota negatively regulate Hnf4a. In support, analysis of genomic architecture in mouse intestinal epithelial cells disclosed that microbiota colonization leads to activation or inactivation of hundreds of enhancers along with drastic genome-wide reduction of HNF4A and HNF4G occupancy. Interspecies meta-analysis suggested interactions

between HNF4A and microbiota promote gene expression patterns associated with human inflammatory bowel diseases. These results indicate a critical and conserved role for HNF4A in maintaining intestinal homeostasis in response to microbiota.

KEY WORDS:

Crohn's disease, ulcerative colitis, cis-regulatory, NR2A1, Angptl4, microbiome

INTRODUCTION

All animals face the fundamental challenge of building and maintaining diverse tissues while remaining sensitive and responsive to their environment. This is most salient in the intestinal epithelium which performs important roles in nutrient absorption and barrier function while being constantly exposed to complex microbial communities (microbiota) and nutrients within the intestinal lumen. The presence and composition of microbiota in the intestinal lumen influence diverse aspects of intestinal development and physiology including dietary nutrient metabolism and absorption, intestinal epithelial renewal, and edification of the host immune system. Abnormal host-microbiota interactions are strongly implicated in the pathogenesis of inflammatory bowel diseases (IBD), including Crohn's disease (CD) and ulcerative colitis (UC) (Sartor and Wu 2016). Studies in mouse and zebrafish models of IBD have established that impaired intestinal epithelial cell (IEC) responses to microbiota are a key aspect of disease progression (Bates et al. 2007; Kamada et al. 2013; Marjoram et al. 2015). Improved understanding of the molecular mechanisms by which microbiota evoke host responses in the intestinal epithelium can be expected to lead to new strategies for preventing or treating IBD and other microbiota-associated diseases.

The ability of IEC to maintain their physiologic functions and respond appropriately to microbial stimuli is facilitated through regulation of gene transcription. Genome-wide comparison of transcript levels in intestinal tissue or isolated IEC from mice reared in the absence of microbes (germ-free or GF) to those colonized with a microbiota (conventionalized or CV) have revealed hundreds of genes that have significantly increased or decreased mRNA levels following microbiota colonization (Camp et al. 2014). Interestingly, many mouse genes that are transcriptionally regulated by microbiota have zebrafish homologs that are similarly responsive, suggesting the existence of evolutionarily-conserved regulatory mechanisms (Rawls et al. 2004). For example, the protein hormone Angiopoetin-like 4 (ANGPTL4, also called FIAF) is

encoded by a single ortholog in the mouse and zebrafish genomes, and microbiota colonization results in significant reductions in transcript levels in the small intestinal epithelium of both host species (Bäckhed et al. 2004; Camp et al. 2012). Whereas these impacts of microbiota on host IEC transcriptomes and their downstream consequences have been extensively documented, the upstream transcriptional regulatory mechanisms remain poorly understood.

Specification and tuning of gene transcription proceeds in part through interactions between transcription factors (TFs) and their sequence-specific binding to *cis*-regulatory DNA. *Cis*-regulatory regions (CRRs) harbor binding sites for multiple activating or repressing TFs and are generally associated with nucleosome depletion and specific post-translational modifications of histone proteins within adjacent nucleosomes when acting as poised (H3K4me1) or active (H3K27ac) enhancers (Creyghton et al. 2010). Antibiotic administration can impact transcript levels and histone modifications in IECs (Thaiss et al. 2016), however it's unclear if these changes are indirect effects caused by alterations to microbiota composition, direct effects of the antibiotic on host cells, or by the effects of remaining antibiotic-resistant microbiota (Morgun et al. 2015). Previous studies have shown that histone deacetylase 3 is required in IECs to maintain intestinal homeostasis in the presence of microbiota (Alenghat et al. 2013), and that overall histone acetylation and methylation in the intestine is altered by microbiota colonization (Krautkramer et al. 2016). However, the direct and specific effects of the microbiota on host CRRs and subsequent transcriptional responses in IECs remain unknown.

Our previous studies predicted key roles for one or more nuclear receptor TFs in microbial down regulation of IEC gene expression (Camp et al. 2014), but the specific TF(s) were not identified. Nuclear receptors are ideal candidate TFs for integrating microbe-derived signals, since for many their transcriptional activity can be positively or negatively regulated by the binding of metabolic or hormonal ligands (Evans and Mangelsdorf 2014). However, the roles of nuclear receptors in host responses remain poorly understood, and no previous study has defined the

impact of microbiota on nuclear receptor DNA binding. Nuclear receptors are a metazoan innovation. The earliest animals encoded a single nuclear receptor orthologous to Hepatocyte nuclear factor 4 (HNF4; nuclear receptor subfamily NR2A) (Bridgham et al. 2010). Despite subsequent duplication and diversification, distinct HNF4 TFs remain encoded in extant animals including mammals (HNF4A, HNF4G) and fishes (Hnf4a, Hnf4b, Hnf4g) (Supplemental Fig. S1G). HNF4A serves particularly important roles in IECs, where it binds CRRs and activates expression of genes involved in IEC maturation and function (Stegmann et al. 2006). IEC-specific knockout of mouse *Hnf4a* results in spontaneous intestinal inflammation similar to human IBD (Darsigny et al. 2009). In accord, genetic variants at human *HNF4A* are associated with risk for both UC and CD as well as colon cancer (Barrett et al. 2009; Jostins et al. 2012; Marcil et al. 2012; Chellappa et al. 2016). HNF4A is predicted to bind a majority of IBD-linked CRRs and to regulate IBD-linked genes (Haberman et al. 2014; Meddens et al. 2016). Similarly, genetic variants near human *HNF4G* have been associated with obesity and CD (Franke et al. 2007; Berndt et al. 2013). Importantly, these diverse roles for HNF4 TFs in host physiology have only been studied in animals colonized with microbiota. Therefore, the role of HNF4 in host-microbiota interactions and the implications for human IBD remain unknown.

RESULTS

hnf4a is essential for transcriptional activity from a microbiota-suppressed cis-regulatory DNA region

To identify transcriptional regulatory mechanisms underlying microbial control of host gene expression, we took advantage of a previously identified microbiota-responsive CRR termed in3.4 located within the third intron of zebrafish *angptl4* (Fig. 1A). A GFP reporter construct under control of in3.4 termed *in3.4:cfos:gfp* drives tissue specific expression of GFP in zebrafish IEC and is suppressed by microbiota colonization, recapitulating the microbial suppression of

zebrafish *angptl4* (Camp et al. 2012). However, the factor(s) that mediate microbial suppression of in3.4 were unknown. Using a yeast one-hybrid (Y1H) assay, we tested the capacity of 150 TFs expressed in the zebrafish digestive system to bind in3.4 (Supplemental Fig. S1A,B; Supplemental Table S1) and detected an interaction only with *hnf4a*, *hnf4b*, and *hnf4g* (Fig. 1B). When either of two predicted Hnf4 motifs in in3.4 are mutated, the Hnf4-in3.4 interaction in the Y1H assay and intestinal GFP expression in *in3.4:cfos:gfp* zebrafish is strongly reduced (Supplemental Fig. S1C-F). Interestingly, while *gata4*, *gata5*, and *gata6* have predicted motifs in in3.4 (Camp et al. 2012) these TFs did not interact in the Y1H assay. This suggests that HNF4 TFs are capable of binding in3.4 directly and HNF4 binding sites are necessary for directing in3.4-based transcription *in vitro* and in the intestine.

We hypothesized that the *hnf4* transcription factor family is required to mediate microbial suppression of in3.4 activity. Although the Y1H assay demonstrated all 3 zebrafish Hnf4 members are capable of binding in3.4, we concentrated our efforts on understanding the function of *hnf4a* because it is the most highly conserved Hnf4 family member (Supplemental Fig. S1G; Supplemental Table S10) and has well-documented roles in intestinal physiology (San Roman et al. 2015). To that end, we generated *hnf4a* mutant zebrafish using the CRISPR/Cas9 system (Fig. 1C; Supplemental Fig. S2A-C,E). Whole-animal *Hnf4a* knockout mice die during early embryogenesis due to failure to develop visceral endoderm (Duncan et al. 1997), but zebrafish and other fishes do not develop that extra-embryonic tissue. We found that zebrafish homozygous for a non-sense mutation in *hnf4a* are viable and survive to sexual maturity (Supplemental Fig. S2D) providing new opportunities to study the roles of HNF4A in host-microbiota interactions.

To determine if *hnf4a* is essential for in3.4 activity, we crossed mutant *hnf4a* alleles to the *in3.4:cfos:gfp* transgenic reporter line. GFP expression was significantly reduced in the absence of *hnf4a* suggesting that *hnf4a* activates in3.4 (Fig. 1D,E,G,H). This loss of GFP expression in

hnf4a$^{-/-}$ mutants was not associated with overt defects in brush border development or epithelial polarity in larval stages (Fig. 1F), nor in the establishment of intestinal folds during adult stages (Fig. 1G). However, intestinal lumen of mutant larvae was reduced in size at 6 days post fertilization (dpf) compared to WT siblings (Fig. 1F; Supplemental Fig. S2F). Together, these data indicate *hnf4a* is essential for robust activity of a microbiota-suppressed CRR. Unlike *in3.4:cfos:gfp*, *angptl4* is expressed in multiple tissues and cell types (Camp et al. 2012). To determine if intestinal *angptl4* expression is dependent on *hnf4a* function, we isolated RNA from IECs from *hnf4a*$^{+/+}$ and *hnf4*$^{-/-}$ adult *in3.4:cfos:gfp* zebrafish and performed qRT-PCR. Adult IECs (AIECs) from *hnf4a*$^{-/-}$ have significant reductions in mRNA for *gfp*, *fabp*2 (a known HNF4A target in human cell lines) (Klapper et al. 2007), and *hnf4a* compared to *hnf4a*$^{+/+}$ controls. However, *angptl4* expression remained unchanged in *hnf4*$^{-/-}$ AIECs compared to WT, suggesting *angptl4* transcript levels in the adult intestine are regulated by additional mechanisms and not solely from in3.4 or Hnf4a (Fig. 1H). Transcript levels for *hnf4g* and *hnf4b* in *hnf4a*$^{-/-}$AIEC were also unchanged. Together, these results establish that Hnf4a is required for in3.4 activity in IECs and raises the possibility that Hnf4a may have broader roles in mediating host transcriptional and physiological responses to microbiota.

Hnf4a activates transcription of genes that are suppressed upon microbiota colonization

To better define the roles of *hnf4a* in microbiota response and other aspects of digestive physiology, we used RNA-seq to compare mRNA levels from digestive tracts isolated from *hnf4a*$^{+/+}$ and *hnf4a*$^{-/-}$ zebrafish larvae in the presence (CV) or absence of a microbiota (GF; Fig. 2A). Consistent with our previous studies (Rawls et al. 2004; Kanther et al. 2011), comparison of wildtype zebrafish reared under CV vs GF conditions revealed differential expression of 598 genes that were enriched for processes such as DNA replication, oxidation reduction, and response to bacterium (Fig. 2B,D; Supplemental Fig. S3D; Supplemental Tables S2, S4). Strikingly, disruption of the *hnf4a* gene caused gross dysregulation of the transcriptional

response to microbiota colonization, with the total number of microbiota responsive genes (CV vs GF) increasing to 2,217. Furthermore, comparison of the *hnf4a* mutant (Mut) vs wild type (WT) genotypes revealed differential expression of many genes in the CV condition (2,741 genes) and GF condition (1,441 genes) that inform a general role for Hnf4a in regulating genes in the intestinal tract (Fig. 2D,E). Principal components analysis (Supplemental Fig. S3A) and hierarchical clustering (Fig. 2B) of FPKM values indicated that *hnf4a* genotype had a complex contribution to regulating genes involved in both responses to the microbiota and digestive physiology.

Because we found that *hnf4a* activates the microbiota-suppressed intestinal CRR, in3.4, we hypothesized that this may represent a general regulatory paradigm for other microbiota-influenced CRRs and genes across the genome. When we compared the 598 genes that were microbiota responsive in wildtype digestive tracts with the 2,741 genes that *hnf4a* regulates in CV digestive tracts we found these lists shared 295 genes that included *fads2* and *saa*, both of which have human orthologs that are either implicated (*FADS1/2*) or markers (*SAA*) of IBD (Plevy et al. 2013; Costea et al. 2014) (Fig. 2C-F). While loss of Hnf4a could be pleiotropic, strikingly, the overlap between these subsets reveals that a disproportionate 88 of the 98 (~90%) microbiota-suppressed genes are activated by *hnf4a* (Fig. 2F; Supplemental Table S2). These 88 genes represent almost half of all 185 genes suppressed by the microbiota. These data suggest, like its role at in3.4, *hnf4a* plays a critical role in directly activating a large percentage of genes that are suppressed by microbial colonization. This set of *hnf4a*-activated microbiota-suppressed genes is enriched for ontologies and pathways involved in lipid and carbohydrate metabolism, suggesting microbiota might regulate these processes through suppression of Hnf4a (Fig. 2G). Interestingly, the top 2 diseases associated with this gene set were obesity-related traits and IBD (Fig. 2G; Supplemental Table S11). Based on these results,

we hypothesized that Hnf4a DNA binding is lost upon microbial colonization within CRRs associated with microbiota-suppressed genes.

HNF4A binding sites are enriched in promoters near genes associated with microbiota-regulated H3K27ac marks

Previous attempts to identify microbial responsive enhancers genome-wide were complicated by the lack of significant changes in chromatin DNase accessibility between GF and CV IECs from mouse colon and ileum (Camp et al. 2014). These previous findings suggested other chromatin dynamics may be involved in regulating the IEC response to microbiota. We therefore sought to provide a genomic context for understanding how the microbiota alter HNF4A activity and chromatin modifications in IECs by performing RNA-seq, DNase-seq, and ChIP-seq for the enhancer histone modifications H3K4me1 and H3K27ac, and the HNF4 TF family members HNF4G and HNF4A in CV and GF conditions totaling 35 datasets. We conducted these experiments in jejunal IEC from gnotobiotic mice because: (1) ChIP-grade antibodies for mouse HNF4A and HNF4G are available, (2) the larger organ size in mice provided sufficient numbers of IECs for ChIP-seq experiments, and (3) we speculated that the roles of HNF4A in host response to microbiota may be conserved to mammals. We first performed DNase-seq in jejunal IEC from mice reared GF or colonized for two weeks with a conventional mouse microbiota (CV) to determine the impact of microbiota colonization on chromatin accessibility (Fig. 3A). In accord with previous studies that tested for chromatin accessibility in ileal or colonic IECs from GF or CV mice (Camp et al. 2014), we similarly found no differential DNase hypersensitivity sites (DHSs) in GF or CV jejunum (data not shown, but see Supplemental Fig. S4A; Supplemental Tables S6, S8). These data indicate that gross accessibility changes in chromatin do not underlie the transcription of microbiota-responsive genes in IECs.

To test if other metrics of chromatin utilization were dynamically regulated by microbiota, we performed ChIP-seq from GF and CV mouse jejunal IECs for histone marks H3K4me1 and

H3K27ac that are enriched at poised enhancers and active enhancers, respectively (Fig. 3B). By determining the single-nearest gene TSS within 10kb of the differential histone marks and overlaying these data with our new RNA-seq datasets, we found that regions that gain poised (H3K4me1) and activated (H3K27ac) enhancers upon colonization are associated with genes that have increased transcript levels upon colonization (Fig. 3C,H-K; Supplemental Fig. S4I; Supplemental Tables S3, S6, S8). Similarly, regions that lose poised and active enhancers upon colonization are associated with microbiota-suppressed genes (Fig. 3C,G,I,J,L; Supplemental Fig. S4J; Supplemental Tables S3, S6, S8). A two-sided Kolmogorov-Smirnov goodness-of-fit test shows a positive relationship between differential H3K4me1/H3K27ac region and increased transcript abundance of nearby genes in the same colonization state (Fig. 3D). Collectively, we identified for the first time a genome-wide map of hundreds of newly identified microbial regulated CRRs, suggesting that microbiota regulation of host genes is mechanistically linked to histone modifications changes more than gross chromatin accessibility changes (Camp et al. 2014).

We leveraged this novel atlas of microbiota-regulated enhancers and accessible chromatin to determine which TFs are predicted to bind to these regions. An unbiased analysis found that three HNF4A binding site motifs were significantly ($p < 1x10^{-45}$, $p < 1x10^{-28}$, and $p < 1x10^{-13}$) enriched in promoters of genes associated with microbiota-suppressed enhancers (Supplemental Fig. S4E), and STAT1 binding site motifs were significantly ($p < 1x10^{-16}$) enriched in promoters of genes associated with microbiota-activated enhancers (Supplemental Fig. S4F). Interestingly, DHS sites associated with differentially active enhancers were enriched for two different sets of TF binding sites. DHSs flanked by microbiota-inactivated enhancers were enriched for nuclear receptor DR1 sites, which can be recognized by HNF4A (Fang et al. 2012), and GATA binding sites ($p = 2.3x10^{-12}$ and $1.1x10^{-6}$ respectively) (Fig. 3E). DHS sites associated with microbiota-activated enhancers were similarly enriched for the nuclear receptor

DR1 binding sites but also for STAT/IRF-like and ETS binding sites ($p = 6.5x10^{-15}$ and $1.3x10^{-17}$ respectively) (Fig. 3F). These data suggest that nuclear receptors like HNF4A may play a central role in IEC responses to microbial colonization.

Microbiota colonization is associated with a reduction in HNF4A and HNF4G cistrome occupancy

To directly evaluate the impact of microbiota on HNF4A activity, we tested the plasticity of the genome wide distribution of HNF4s in response to microbial colonization. HNF4A bound 28,901 sites and HNF4G bound 21,875 sites across the genome in GF conditions in jejunal IECs with ~80% of these sites being bound by both TFs. In striking contrast, the number of sites bound by HNF4A and HNF4G in CV conditions was ~10 fold less (Fig. 4A,B; Supplemental Fig. S5A-D; Supplemental Tables S5, S8). Of the 3,964 HNF4A binding sites detected in CV there were only 267 HNF4A sites that were specific to the CV condition (Supplemental Fig. S6A,C; Supplemental Table S8). Yet, the genes associated with these HNF4A sites that are retained in CV are enriched for ontologies and pathways fundamental to intestinal epithelial biology (Supplemental Fig. S6B). Surprisingly, we found HNF4A sites are equally distributed between genes that are upregulated in both GF and CV conditions (Supplemental Fig. S6E). However, we did find that the average CV HNF4A signal strength was significantly increased at HNF4A sites associated with microbiota-induced genes relative to those HNF4A sites associated with microbiota-suppressed genes, suggesting HNF4A may play a limited role in genes upregulated by colonization (Supplemental Fig. S6F). In contrast, GF HNF4A ChIP signal was equivalent at HNF4A sites associated with microbiota-suppressed and induced genes (Supplemental Fig. S6F). Interestingly, we found that HNF4A sites correspond with increased H3K27ac, H3K4me1 and DHS signal in GF compared to these same chromatin marks in CV (Supplemental Fig. S6G). We do not believe that the reduction of HNF4A binding is the result of chromatin quality in a particular condition since there are genomic locations where GF and CV HNF4A sites

appeared to have equivalent signal (Fig. 4C). Furthermore, ChIP enrichment in these IEC preparations for another zinc finger TF, CTCF, was unaffected by microbiota colonization (Supplemental Fig. S6D). This indicates that the observed reduction of Hnf4 ChIP signal in CV IECs is a result of microbiota on HNF4 binding, and is not the result of altered ChIP efficiency or sample quality in the different conditions. To test if microbial suppression of HNF4A occupancy is persistent, we performed ChIP-PCR from ex-GF mice that were colonized with microbiota for 6, 15 or 45 days. We found that even after 45 days post-colonization, HNF4A occupancy at binding sites was significantly reduced compared to GF (Fig. 4F). The dramatic loss of HNF4A and HNF4G DNA binding upon colonization is consistent with HNF4A acting as a potent activator of microbiota-suppressed genes.

We further speculated that certain coregulatory sequence-specific transcription factors may also contribute to regulating transcription with HNF4 at these sites. To explore this possibility, we searched for TF motifs associated with HNF4A ChIP sites and found an enrichment of putative binding sites for TFs known to be involved in small intestinal physiology (GATA and HOXC9) as well as nutrient metabolism (PDX1) at both HNF4A bound regions associated with genes and enhancers suppressed by microbes (Fig. 4D). We similarly found GATA sites located within an HNF4A-bound CRR near murine *Angptl4* (Fig. 4E), similar to the coincident HNF4 and GATA motifs in in3.4 (Camp et al. 2012). Furthermore, binding sites for TFs known to be involved in cell proliferation and cell death (ETS transcription factor family) are enriched near HNF4A bound regions that intersect microbiota-induced enhancers (Fig. 4D). Collectively our integrative analyses of these novel ChIP-seq, DNase-seq, and RNA-seq datasets identifies a core set of putative microbiota-responsive TFs that may interact with HNF4A to mediate microbial control of IEC gene expression. These results suggest HNF4A plays a major role in integrating microbial signals to regulate gene expression, and raise the possibility that this novel microbiota-HNF4A axis might contribute to human disease.

Microbiota-mediated suppression of HNF4A may contribute to gene expression profiles associated with human IBD

Both HNF4A and the intestinal microbiota have been separately implicated in the pathogenesis of the human IBDs Crohn's disease (CD) and ulcerative colitis (UC) (Ahn et al. 2008; Sartor and Wu 2016). However, a mechanistic link between microbiota and HNF4A in the context of IBD pathogenesis has not been established. Previous transcriptomic studies have identified genes differentially expressed in ileal (iCD) and colonic CD (cCD) and UC (Arijs et al. 2009; Haberman et al. 2014) biopsies. We queried these human gene lists to identify one-to-one orthologs in mice, and referenced them against our new gnotobiotic mouse jejunal HNF4A ChIP-seq data (Fig. 5A). Strikingly, the majority of human genes downregulated in each of these IBD datasets have mouse orthologs that are associated with an HNF4A-bound region (Fig. 5B,C; Supplemental Table S7). Focusing on the iCD dataset from the largest of these previous studies (Haberman et al. 2014), we found differential iCD genes associated with HNF4A sites are enriched for distinct ontologies and pathways that are dysregulated in IBD (Fig. 5H-K). In contrast to IBD, analysis of intestinal transcriptomic datasets from human subjects with necrotizing enterocolitis (NEC) (Tremblay et al. 2016) or insulin-resistance (IR) (Veilleux et al. 2015) did not reveal strong enrichment of HNF4A-bound regions near downregulated genes (Fig. 5C). Notably, in each of these CD, UC, NEC, and IR datasets, a greater percentage of downregulated genes were linked to HNFA-bound regions compared to upregulated genes (Fig. 5B). These data suggest microbiota-dependent and microbiota-independent suppression of HNF4A activity in the intestine might play an important role in IBD pathologies. To assess if microbiota suppression of HNF4A activity regulates genes differentially expressed in IBD, we queried the published human IBD and NEC gene expression datasets to identify human-mouse-zebrafish one-to-one-to-one orthologs that were differentially expressed in our RNA-seq analysis of gnotobiotic zebrafish *hnf4a* mutants (Fig. 5D). We found ortholog expression fold

changes in human IBD/healthy comparisons most closely resembled the expression fold changes of MutCV/MutGF and MutCV/WTCV (Fig. 5E-G). Neither the WTCV/WTGF nor the MutGF/WTGF comparisons faithfully recapitulate the expression profiles of IBD/healthy comparisons. This indicates that both the microbiota and loss of *hnf4a* function in zebrafish are necessary to induce a gene expression profile that resembles human IBD. Strikingly, the positive correlation and significant resemblance to the iCD-like gene signatures in the colonized *hnf4a*$^{-/-}$ compared to colonized *hnf4a*$^{+/+}$ zebrafish digestive tracts become even stronger when we limited our analysis to one-to-one orthologs that have an association with an HNF4A bound region in mouse IECs (Fig. 5G). Together, these results indicate that intestinal suppression of HNF4A target genes is a prevalent feature of human CD and UC, and suggests a model wherein HNF4A maintains transcriptional homeostasis in the presence of a microbiota and protects against an evolutionarily-conserved IBD-like gene expression signature.

DISCUSSION

Over the course of animal evolution, the intestinal epithelium has served as the primary barrier between animal hosts and the complex microbial communities they harbor. IECs maintain this barrier and perform their physiological roles in nutrient transport and metabolism through dynamic transcriptional programs. The regulatory mechanisms that orchestrate these transcriptional programs represent potential therapeutic targets for a variety of human intestinal diseases including IBD. Here we discovered that HNF4A activity and its transcriptional network are suppressed by microbiota. HNF4A is the oldest member of the nuclear receptor TF family (Bridgham et al. 2010), and our findings in fish and mammals suggest that microbial suppression of HNF4A may be a conserved feature of IEC transcriptional programs present in the common ancestor.

We discovered HNF4A as a microbiota-suppressed transcription factor by demonstrating it specifically binds to a microbiota-suppressed *cis*-regulatory element, in3.4, which is located at the zebrafish gene *angptl4*. This finding combined with our zebrafish RNA-seq data (Fig. 2FG) revealed a broad role for HNF4A in activation of microbially-suppressed transcripts. Though *hnf4a* mutant zebrafish have reduced in3.4 activity in the intestinal epithelium based on transgenic reporter assays, the transcript levels of the endogenous zebrafish *angptl4* gene appears unaffected in both larval digestive tracts and adult IECs. The zebrafish genome encodes two additional HNF4 family members (*hnf4b*, *hnf4g*), and previous studies in mammals have shown *Angptl4* can be regulated by other metabolically-activated nuclear receptors (Staiger et al. 2009; Korecka et al. 2013). We hypothesize that loss of HNF4A function may lead to a metabolic imbalance leading to atypical or compensatory activation of other *trans*- and *cis*-factors that control expression of *angptl4* and other genes in the intestine.

Our results suggest new links between HNF4A and microbiota in the context of human IBD. IBD patients, particularly those suffering from Crohn's disease, often present with decreased serum low-density lipoprotein levels and reduced total cholesterol levels compared to healthy individuals (Hrabovsky et al. 2009; Agouridis et al. 2011). These serum levels are consistent with reduced transcript levels for genes involved in intestinal absorption and transport of lipid and cholesterol in ileal and colonic biopsies from UC and CD patients (Arijs et al. 2009; Haberman et al. 2014). Transcription factors, including nuclear receptors like HNF4A and FXR, are known to regulate bile acid production, lipid and cholesterol absorption and have already been implicated in IBD (Ahn et al. 2008; Nijmeijer et al. 2011). Previous studies have shown that some IBD-associated H3K27ac activated regions that also overlap with an IBD-associated SNP contain HNF4A binding sites (Mokry et al. 2014). This is consistent with our findings and supports a role for HNF4A in regulating gene expression and inflammation in the context of IBD. However, our work is the first to demonstrate a role for microbiota in suppressing HNF4A, and

to implicate microbiota-HNF4A interactions in driving an IBD-like gene expression signature (Fig. 5). In addition to IBD, human *HNF4A* variants are associated with metabolic syndrome (Weissglas-Volkov et al. 2006) and type 2 diabetes (Ma et al. 2016). Interestingly, microbiota have also been implicated in both of these diseases (Qin et al. 2012; Vrieze et al. 2012) raising the possibility that microbiota suppression of HNF4A *trans* activity could play a role in these diseases as well. Indeed, we find that genes down regulated in intestinal tissue from IR obese patients have increased HNF4A binding associations compared to up-regulated genes (Veilleux et al. 2015), similar to the enrichment of HNF4A associations at down-regulated genes in IBD (Fig. 5B,C). Interestingly, up-regulated genes in these IR-obese patients were enriched for pro-inflammatory markers. This underscores the relationship between metabolic impairments and inflammation in the intestine, and prompts further investigation of how HNF4A might contribute. HNF4A has been shown to play key roles in anti-oxidative and anti-inflammatory defense mechanisms (Marcil et al. 2010) so aberrant microbial suppression could promote an inflammatory state. HNF4A target genes are downregulated in human IBD (Arijs et al. 2009; Haberman et al. 2014) and mouse experimental colitis (Chahar et al. 2014), and the HNF4A target *APOA1* has been shown to be protective against intestinal inflammation in mice (Gkouskou et al. 2016). We speculate that the genes governed by this novel microbiota-HNF4A axis may include additional anti- and pro-inflammatory factors that could provide new targets for IBD therapy.

Our results reveal similar effects of microbiota colonization and experimental colitis on HNF4A cistrome occupancy in the intestine, but the underlying molecular mechanisms are unresolved. DSS induced colitis results in reduced HNF4A protein levels and altered cellular localization (Chahar et al. 2014), however our results indicate the microbiota neither reduce HNF4A protein levels nor impact its nuclear localization in jejunal IECs two weeks after colonization (Supplemental Fig. 65H,I). Colonization of GF mice with microbiota initiates a transcriptional

adaptation in the intestine that progresses for several weeks before reaching homeostasis (El Aidy et al. 2012). However, our data indicate HNF4A suppression is achieved within 15 days and persists through at least 45 days after colonization. These data collectively suggest that microbiota suppress HNF4A activity in the jejunum through mechanisms distinct from those utilized in DSS induced colitis.

HNF4A has been characterized as a master metabolic regulator for its conserved roles in gluconeogenesis, glucose homeostasis, and fatty acid metabolism (Palanker et al. 2009; Frochot et al. 2012; Barry and Thummel 2016). Despite its clear importance in metabolic health, relatively little insight into its regulation in a biological context has been reported. *In vitro* and cell culture studies have identified possible suppressors and activators of HNF4A including acetylation by CREB-binding protein (CBP), which has been shown to induce HNF4A activity (Soutoglou et al. 2000; Hong et al. 2003). The nuclear receptor cofactor and master regulator of mitochondrial biogenesis PGC-1A binds HNF4A and promotes activation of HNF4A target genes (Rha et al. 2009). Colonization of GF animals with a microbiota leads to increased energy harvest (Rabot et al. 2010; Semova et al. 2012) and changes in metabolic homeostasis including decreased AMPK activity in skeletal muscle and liver (Backhed et al. 2007). AMPK activates PGC-1A (Jager et al. 2007), therefore, microbiota might suppress HNF4A activity indirectly through induced alterations in metabolic homeostasis. Other studies have shown that HNF4A activity is controlled through use of alternative promoters which generate different isoforms (Huang et al. 2009). However, we did not detect differential *Hnf4a* exon usage by DEXseq (Li et al. 2015) in our RNA-seq data from GF and CV IECs (data not shown). Another facet of HNF4A biology that remains unresolved is the identity of its endogenous ligand(s). Although historically considered an orphan nuclear receptor, several fatty acids, including linoleic acid, have been identified as ligands for HNF4A (Hertz et al. 1998; Palanker et al. 2009; Yuan et al. 2009). Fatty acids are an attractive class of putative regulators of HNF4A since the

microbiota are known to regulate FA absorption in zebrafish IECs (Semova et al. 2012). Further, specific bacterial taxa are known to modify the structure of polyunsaturated FAs (PUFAs) and these native and modified PUFAs have distinct impacts on animal health (O'Shea et al. 2012) and may serve as therapeutics for IBD (Mbodji et al. 2013).

In our attempt to understand how the microbiota regulate HNF4A activity and host gene transcription, we were motivated to investigate if microbiota impact histone modification and chromatin accessibility in the mouse jejunum. Our findings support the model that microbiota alter IEC gene expression by affecting TF binding and histone modification at tissue-defined open chromatin sites (Camp et al. 2014). We provide the genomic addresses of hundreds of microbiota-regulated enhancers as well as the genes associated with these enhancers and HNF4A binding sites. Similar to other findings in intraepithelial lymphocytes (Semenkovich et al. 2016), our work demonstrates a clear microbial contribution to the modification of the histone landscape in IECs and provides another important layer of regulation that orchestrate microbiota regulation of host genes involved in intestinal physiology and human disease. We were also able to establish a link between microbiota-regulated genes and enhancers and NR binding sites. These NR binding sites are coincident with a core set of TFs that are enriched near microbiota-suppressed enhancers/genes (GATA) or induced enhancers/genes (ETS-factors and IRF) (Supplemental Fig. S7). GATA4 was previously shown to be a positive regulator of genes suppressed by microbiota in the mouse jejunum (Shulzhenko et al. 2011), supporting potential coregulatory interactions with HNF4A. Coregulation by other TFs represents one possible mode of HNF4A regulation by which the microbiota could suppress HNF4A activity without impacting the gene transcription of all HNF4A -associated genes.

METHODS

Yeast 1-Hybrid ORFeome Screen:

The yeast 1-hybrid ORFeome screen was performed using the Clontech MatchmakerTM Gold Yeast One-hybrid Library Screening System (cat. 630491) protocol with the following exceptions: The Y1HGold yeast strain was transformed using standard yeast transformation procedures with BstBI digested pBait-AbAi containing either the WT or a SDM in3.4 or the p53 binding site sequence, and positive transformants were selected on SD/-URA media. In addition, a ORFeome library consisting of 148 zebrafish transcription factors cloned from adult zebrafish liver (Supplemental Table S1) into pDEST22 prey vectors containing an N-terminal GAL4-activation domain was utilized (Boyle et al. 2017). For additional information, see Supplemental Methods.

Mouse IEC Isolation for DNAse, ChIP and RNA-seq:

The small intestine was removed from the mouse and the jejunum was excised from the duodenum and ileum. Duodenum was defined as the anterior 5 cm of the midgut and ileum was defined as posterior 6 cm of midgut as described (Camp, et al 2014). Adipose and vasculature were removed from the tissue. The jejunum was opened longitudinally along the length of the tissue, exposing the lumen and epithelial cell layer. Luminal debris was washed away from the epithelia with ice cold sterile PBS. The tissue was temporarily stored in 10 ml of ice cold sterile PBS with 1x Protease Inhibitor (Complete EDTA-Free, Roche 1187350001) and 10 uM Y-27632 (ROCK I inhibitor, Selleck Chemicals S1049) to inhibit spontaneous apoptosis. The jejunum was moved into a 15 ml conical tube containing 3 mM EDTA in PBS with 1x protease inhibitor and 10 uM Y-27632. The tissue was placed on a nutator in a cold room for 15 minutes. The jejunum was removed from the 3 mM EDTA and placed on an ice cold glass petri dish with PBS containing 1mM MgCl2 and 2 mM CaCl2 with protease inhibitors and 10 uM Y-27632. Villi were scraped off of the tissue using a sterile plastic micropipette and placed into a new 15 ml conical tube. The isolated IECs were then crosslinked for ChIP or used for DNAse-seq or RNA-seq. For additional information, see Supplemental Methods.

Bioinformatic and Statistical analysis:

Sample sizes for zebrafish experiments (noted in figure legends) were selected based on genotype availability and transgenesis efficiency. All sample collection was performed two or more times on independent days. For sequencing experiments, statistical calls for differential gene expression were made by Cuffdiff2 (Trapnell et al. 2013). For the zebrafish RNA-seq experiment, Next-Gen sequencing was performed once and at the same time to avoid batch effects: WTGF and WTCV (n = 3); MutGF and MutCV (n = 2). We originally collected n = 3 MutGF and MutCV biological replicates, however, using pre-established criteria and to avoid RNA contamination, we excluded one biological replicate from all analysis from these groups because of sequencing reads that mapped within the deleted *hnf4a* exon in the *hnf4a*$^{-/-}$ genotype.

GF mice were randomly chosen by gnotobiotic staff for microbiota colonization (CV) based on their availability and litter sizes. All sample collection was performed two or more times per condition on independent days. GF and CV mouse samples were collected on different days. For sequencing experiments, statistical calls for differential gene expression and differential peak calls were made by Cuffdiff2, MACS2, and DESeq2 (Zhang et al. 2008; Anders and Huber 2010; Trapnell et al. 2013; Love et al. 2014). For the mouse RNA-seq experiment Next-Gen sequencing was performed once and at the same time to avoid batch effects: GF (n = 2) and CV (n = 2). Paired GF and CV ChIP and library amplification was performed simultaneously. Typically, biological ChIP replicates were sequenced on different days and were always paired with the other condition (i.e. CV and GF were always sequenced together). The number of biological ChIP replicates (noted in figure legends) was dependent on reproducibility between ChIP samples and/or our ability to determine statistical differential sites using DESeq2 (for H3K4me1 and H3K27ac).

All statistical metrics (except where otherwise noted) were performed in Graphpad Prism 7.01. Deming linear regression was used for Fig. 5 because it is a stronger and more accurate assessment of correlation when both the x and y variables have experimental error. Details regarding the other statistical tests used in this study can be found in the figure legends or above.

For detailed methods on animal husbandry, zebrafish transgenesis, zebrafish mutagenesis, imaging, immunostaining, site-directed mutagenesis, ChIP-, RNA-, and DNase-seq preparation and analysis please see Supplemental Methods.

DATA ACCESS

Transcription factor ChIP-seq, Histone ChIP-seq, DNase-seq and RNA-seq datasets have been submitted to the NCBI Gene Expression Omnibus (GEO; http://www.ncbi.nlm.nih.gov/geo/) under accession number GSE90462.

ACKNOWLEDGEMENTS

We thank Balfour Sartor, Scott Magness, Maureen Bower, Jeremy Herzog, and Scott T. Espenschied for assistance with gnotobiotic mice, and Wenbiao Chen and Stacy Horner for sharing reagents. We also thank the Genomic Sequencing Laboratory at HudsonAlpha Institute for Biotechnology and the Duke Sequencing and Genomic Technologies Facility. This work was supported by grants from the National Institutes of Health (R01-DK081426, U24-DK097748, P01-DK094779, R24-OD016761, and P30-DK34987).

FIGURE LEGENDS

FIGURE 1. Zebrafish *hnf4a* is required for robust *in3.4:cfos:gfp* activity

(A) Schematic of the microbiota-suppressed zebrafish enhancer, in3.4, highlighting the regions required for intestinal activity (purple) which both contain putative HNF4 binding sites (Site 1 and Site 2) (Camp et al. 2012). (B) Image of 4 plates from the Y1H assay showing the *hnf4* family of transcription factors capable of binding in3.4 and driving expression of the antibiotic resistance reporter gene. (C) $Hnf4a^{+/+}$ and $Hnf4a^{-/-}$ protein cartoons showing the DNA binding domain (DBD) and hinge domain (HD). We characterized the two with the largest lesions, a -43 deletion in the hinge domain and a +25 insertion in the hinge domain, which both result in frame-shift early-stop codons and significantly reduced transcript. (D) Stereofluorescence GFP and bright field microscopy showing representative *hnf4a*$^{+/+}$ (top 3) and *hnf4a*$^{-/-}$ (bottom 3) 6dpf *in3.4:cfos:gfp* zebrafish. Genotype was blinded and samples were arranged by intensity of GFP fluorescence. (E) GFP fluorescence (mean ± sem) in *hnf4a*$^{+/+}$ (n = 8), *hnf4a*$^{+/-}$ (n = 8) and *hnf4a*$^{-/-}$ (n = 8) 6dpf *in3.4:cfos:gfp* zebrafish (Two-tailed *t*-test: $t = 17.84, 16.51$, respectively, df = 14, and **** $p < 0.0001$). (F) Confocal microscopy showing representative axial cross sections in 6dpf *hnf4a*$^{+/+}$ (n = 4) and *hnf4a*$^{-43/-43}$ (n = 4) larval zebrafish. 4e8 antibody (yellow) labels the intestinal brush border, DAPI (blue) and phalloidin (red), and nephros (n). (G) Bright field microscopy (top) and stereofluorescence GFP (bottom) for representative *hnf4a*$^{+/+}$ (n = 3) (left) and *hnf4a*$^{-/-}$ (n = 3) (right) dissected intestinal folds from adult *in3.4:cfos:gfp* zebrafish. (H) Relative mRNA levels (mean ± sem) in *hnf4a*$^{+/+}$ (n = 3) and *hnf4a*$^{-/-}$ (n = 3) adult zebrafish intestinal epithelial cell as measured by qRT-PCR. Two-tailed *t*-test: $t = 0.93, 5.22, 6.56, 10.65, 0.75, 0.94$ respectively, df = 4, and * $p < 0.05$, *** $p < 0.001$). See also Supplemental Figures S1 and S2.

FIGURE 2. Hnf4a activates the majority of coregulated genes that are suppressed by the microbiota

(A) Schematic showing the experimental timeline for zebrafish digestive tract GF and CV *hnf4a*$^{+/+}$ and *hnf4a*$^{-/-}$ RNA-seq experiment (n = 3 for WTCV and WTGF and n = 2 for MutCV and MutGF). (B) Hierarchical relatedness tree and heatmap of differentially regulated genes in mutant and gnotobiotic zebrafish digestive tracts. Gene averaged $\log_{10}$ FPKMs for the biological replicates are represented for each of the 4,007 differentially regulated genes. (C) Representative RNA-seq signal tracks at *fatty acid-desaturase 2 (fads2)*, *serum amyloid a (saa)* loci. (D) Summary of the total number of differentially expressed genes between indicated conditions (GF and CV) and genotype (WT and *hnf4a*$^{-/-}$ (Mut)). (E) 4-way Venn diagram showing overlaps between all 4,007 differentially regulated genes. (F) The 295 coregulated genes were plotted using the $\log_2$(FC) calculated in the WTGF/WTCV comparison (X-axis) and WTCV/MutCV (Y-axis). The 88 out of 98 genes that are activated by *hnf4a* but suppressed by the microbiota are highlighted (red) and (G) their GO term, KEGG pathway and disease associations are listed. See also Supplemental Figure S3.

FIGURE 3. Microbiota selectively induce enhancer activity near genes that are upregulated upon microbiota colonization

(A) Schematic showing the gnotobiotic experimental timeline for testing mRNA levels and chromatin architecture in GF and CV. (B) MA plots from DESeq2 analysis (FDR < 0.01) of H3K4me1 (n = 3 per condition) (left) and H3K27ac (n = 2 per condition) (right) ChIP-seq from GF and CV mouse jejunal IECs. Colored dots signify regions significantly enriched for a histone mark in GF (blue) or CV (orange). We found 4,579 unique H3K4me1 and 1,354 unique H3K27ac peaks in GF and 5,155 unique H3K4me1 and 893 unique H3K27ac peaks in CV. (C) Volcano plots showing pairwise comparison of RNA expression between GF (n = 2) and CV (n = 2) jejunal IECs. Blue and orange dots represent genes associated with a region enriched for

H3K4me1 (left) or H3K27ac (right) signal in GF or CV. (D) Two-sided Kolmogorov-Smirnov goodness-of-fit test shows a positive relationship on average between the presence of a region enriched for H3K4me1/H3K27ac signal in a specific colonization state and increased transcript abundance of a neighboring gene in that same colonization state. (E) Top *de novo* binding site motifs found in DHSs that are flanked by regions enriched with H3K27ac signal in GF (E) or CV (F). Representative ChIP-seq tracks highlighting a microbiota-regulated gene associated with differential histone marks in GF (G) (*Akr1c19*, Aldo-keto reductase 1c19) or CV (H) (*Ubd*, Ubiquitin D). Heatmaps showing the average GF and CV H3K4me1 (I) or H3K27ac (J) signal at the 1000 bp flanking differential sites. (K-L) GO terms and KEGG pathways enriched in genes associated with differential H3K27ac sites shown in J. See also Supplemental Figure S4.

FIGURE 4. Microbiota colonization results in extensive loss of HNF4A and HNF4G DNA binding in IEC

(A) Heatmaps showing the average GF and CV ChIP-seq or DNase-seq signal at the 1000 bp flanking HNF4A sites found in GF.(B) Line plots showing the average GF (light-colored line) and CV (dark-colored line) ChIP-seq and DNase-seq RPKM-normalized signal for the indicated TF, histone mark or DHS at the 1000 bp flanking HNF4A sites found in GF (HNF4A: n = 3 per condition; HNF4G: n = 4 per condition; H3K27ac n = 2 per condition; H3K4me1: n = 3 per condition; DNase: n = 3 for CV, n = 2 for GF) . (C) Representative signal tracks highlighting a microbiota-induced gene (*Pigr*, Polymeric immunoglobulin receptor) that is associated with an HNF4A peak with similar signal in both GF and CV jejunal IECs. (D) Heatmap showing the enrichment of TFBS motifs within 50 bp of the DHS or HNF4A peak maxima. (E) Representative signal track at *Angptl4* highlighting two GATA4 sites within an HNF4A bound region. (F) Bar graph showing HNF4A ChIP-PCR results at *Angptl4*, *Apoa1* and *Pck1* loci from jejunal IECs from mice colonized for 0 (n = 2), 6 (n = 3), 15 (n = 2) and 45 (n = 3) days. Data are relative to

568 the GF condition and normalized against a negative control locus (*Neurog1*) * p < 0.5, ** p <
569 0.005, *** p < 0.0005. See also Supplemental Figures S5 and S6.

570 **FIGURE 5. Microbiota suppression of HNF4A activity is highly correlated with genes and**
571 **intestinal processes suppressed in human IBD and conserved in zebrafish**

572 (A) Flow chart showing the experimental design and filters used to identify IBD, NEC, or IR gene
573 orthologs associated with mouse HNF4A ChIP sites. (B) Bar chart showing the proportion of
574 HNF4A associations in GF and CV mouse jejunal IECs near human-to-mouse one-to-one gene
575 orthologs differentially regulated in human pediatric ileal Crohn's Disease (iCD-1), adult iCD
576 (iCD-2), adult colonic Crohn's Disease (cCD), adult ulcerative colitis (UC), neonatal necrotizing
577 enterocolitis (NEC) or insulin-resistance (IR). (C) Heatmap representing the $-\text{Log}_{10}$ (p-value) of
578 the enrichment of GF or CV HNF4A associated genes that are differentially regulated genes in
579 the indicated IBD datasets. Log_{10} p-values were calculated using a hypergeometric enrichment
580 analysis and converting all HNF4A ChIP associated mouse genes to human orthologs (GF =
581 5863 genes and CV = 2119 genes). (D) Flow chart showing the experimental design and filters
582 used to identify correlations between gnotobiotic WT or mutant zebrafish gene expression and
583 gene orthologs differentially expressed in human IBD or NEC. Because loss of *hnf4a* function in
584 zebrafish appeared to more closely resemble iCD signature than cCD or UC, we performed
585 pairwise comparisons of gene orthologs that are (1) differentially regulated in human iCD and
586 (2) have a mouse HNF4A ChIP association. Example of Deming linear regression analysis
587 showing the correlation of Log_2 (FC) between WTCV/WTGF (E) or MutCV/WTCV (F) zebrafish
588 and pediatric iCD or NEC. m = slope of the line. (G) Heatmap representing slopes of Deming
589 linear regression lines showing positive correlative relationships between the $\log_2$ gene
590 expression fold changes of one-to-one orthologs from human diseases compared to $\log_2$ fold
591 changes in zebrafish WTCV/WTGF, MutCV/MutGF, MutCV/WTCV, and MutGF/WTGF. Hash
592 signs indicate slope of Deming linear regression lines is significantly greater than WTCV/WTGF

comparison (#, $p < 0.05$; ##, $p < 0.0001$). Asterisks indicate slope of Deming linear regression line is significantly greater than MutGF/WTGF (*, $p < 0.05$; **, $p < 0.001$). Solid boxes correspond to slope of lines in panel 5D, and dashed boxes correspond to slope of lines in panel 5E. (H-K) The top 5 GO terms and the top 5 KEGG pathways for indicated gene lists.

REFERENCES

Agouridis AP, Elisaf M, Milionis HJ. 2011. An overview of lipid abnormalities in patients with inflammatory bowel disease. *Ann Gastroenterol* **24**: 181-187.

Ahn SH, Shah YM, Inoue J, Morimura K, Kim I, Yim S, Lambert G, Kurotani R, Nagashima K, Gonzalez FJ et al. 2008. Hepatocyte nuclear factor 4alpha in the intestinal epithelial cells protects against inflammatory bowel disease. *Inflamm Bowel Dis* **14**: 908-920.

Alenghat T, Osborne LC, Saenz SA, Kobuley D, Ziegler CG, Mullican SE, Choi I, Grunberg S, Sinha R, Wynosky-Dolfi M et al. 2013. Histone deacetylase 3 coordinates commensal-bacteria-dependent intestinal homeostasis. *Nature* **504**: 153-157.

Anders S, Huber W. 2010. Differential expression analysis for sequence count data. *Genome Biol* **11**: R106.

Arijs I, De Hertogh G, Lemaire K, Quintens R, Van Lommel L, Van Steen K, Leemans P, Cleynen I, Van Assche G, Vermeire S et al. 2009. Mucosal gene expression of antimicrobial peptides in inflammatory bowel disease before and after first infliximab treatment. *PLoS One* **4**: e7984.

Bäckhed F, Ding H, Wang T, Hooper LV, Koh GY, Nagy A, Semenkovich CF, Gordon JI. 2004. The gut microbiota as an environmental factor that regulates fat storage. *Proc Natl Acad Sci U S A* **101**: 15718-15723.

Backhed F, Manchester JK, Semenkovich CF, Gordon JI. 2007. Mechanisms underlying the resistance to diet-induced obesity in germ-free mice. *Proc Natl Acad Sci U S A* **104**: 979-984.

Barrett JC, Lee JC, Lees CW, Prescott NJ, Anderson CA, Phillips A, Wesley E, Parnell K, Zhang H, Drummond H et al. 2009. Genome-wide association study of ulcerative colitis identifies three new susceptibility loci, including the HNF4A region. *Nat Genet* **41**: 1330-1334.

Barry WE, Thummel CS. 2016. The Drosophila HNF4 nuclear receptor promotes glucose-stimulated insulin secretion and mitochondrial function in adults. *Elife* **5**.

Bates JM, Akerlund J, Mittge E, Guillemin K. 2007. Intestinal alkaline phosphatase detoxifies lipopolysaccharide and prevents inflammation in zebrafish in response to the gut microbiota. *Cell Host Microbe* **2**: 371-382.

Berndt SI Gustafsson S Magi R Ganna A Wheeler E Feitosa MF Justice AE Monda KL Croteau-Chonka DC Day FR et al. 2013. Genome-wide meta-analysis identifies 11 new loci for anthropometric traits and provides insights into genetic architecture. *Nat Genet* **45**: 501-512.

Boyle G, Richter K, Priest HD, Traver D, Mockler TC, Chang JT, Kay SA, Breton G. 2017. Comparative Analysis of Vertebrate Diurnal/Circadian Transcriptomes. *PLoS One* **12**: e0169923.

Bridgham JT, Eick GN, Larroux C, Deshpande K, Harms MJ, Gauthier ME, Ortlund EA, Degnan BM, Thornton JW. 2010. Protein evolution by molecular tinkering: diversification of the nuclear receptor superfamily from a ligand-dependent ancestor. *PLoS Biol* **8**.

634 Camp JG, Frank CL, Lickwar CR, Guturu H, Rube T, Wenger AM, Chen J, Bejerano G,
635 Crawford GE, Rawls JF. 2014. Microbiota modulate transcription in the intestinal epithelium
636 without remodeling the accessible chromatin landscape. *Genome Res* **24**: 1504-1516.

637 Camp JG, Jazwa AL, Trent CM, Rawls JF. 2012. Intronic cis-regulatory modules mediate tissue-
638 specific and microbial control of angptl4/fiaf transcription. *PLoS Genet* **8**: e1002585.

639 Chahar S, Gandhi V, Yu S, Desai K, Cowper-Sal-lari R, Kim Y, Perekatt AO, Kumar N,
640 Thackray JK, Musolf A et al. 2014. Chromatin profiling reveals regulatory network shifts and a
641 protective role for hepatocyte nuclear factor 4alpha during colitis. *Mol Cell Biol* **34**: 3291-3304.

642 Chellappa K, Deol P, Evans JR, Vuong LM, Chen G, Briancon N, Bolotin E, Lytle C, Nair MG,
643 Sladek FM. 2016. Opposing roles of nuclear receptor HNF4alpha isoforms in colitis and colitis-
644 associated colon cancer. *Elife* **5**.

645 Costea I, Mack DR, Lemaitre RN, Israel D, Marcil V, Ahmad A, Amre DK. 2014. Interactions
646 between the dietary polyunsaturated fatty acid ratio and genetic factors determine susceptibility
647 to pediatric Crohn's disease. *Gastroenterology* **146**: 929-931.

648 Creyghton MP, Cheng AW, Welstead GG, Kooistra T, Carey BW, Steine EJ, Hanna J, Lodato
649 MA, Frampton GM, Sharp PA et al. 2010. Histone H3K27ac separates active from poised
650 enhancers and predicts developmental state. *Proc Natl Acad Sci U S A* **107**: 21931-21936.

651 Darsigny M, Babeu JP, Dupuis AA, Furth EE, Seidman EG, Levy E, Verdu EF, Gendron FP,
652 Boudreau F. 2009. Loss of hepatocyte-nuclear-factor-4alpha affects colonic ion transport and
653 causes chronic inflammation resembling inflammatory bowel disease in mice. *PLoS One* **4**:
654 e7609.

655 Duncan SA, Nagy A, Chan W. 1997. Murine gastrulation requires HNF-4 regulated gene
656 expression in the visceral endoderm: tetraploid rescue of Hnf-4(-/-) embryos. *Development* **124**:
657 279-287.

658 El Aidy S, van Baarlen P, Derrien M, Lindenbergh-Kortleve DJ, Hooiveld G, Levenez F, Dore J,
659 Dekker J, Samsom JN, Nieuwenhuis EE et al. 2012. Temporal and spatial interplay of
660 microbiota and intestinal mucosa drive establishment of immune homeostasis in
661 conventionalized mice. *Mucosal Immunol* **5**: 567-579.

662 Evans RM, Mangelsdorf DJ. 2014. Nuclear Receptors, RXR, and the Big Bang. *Cell* **157**: 255-
663 266.

664 Fang B, Mane-Padros D, Bolotin E, Jiang T, Sladek FM. 2012. Identification of a binding motif
665 specific to HNF4 by comparative analysis of multiple nuclear receptors. *Nucleic Acids Res* **40**:
666 5343-5356.

667 Franke A, Hampe J, Rosenstiel P, Becker C, Wagner F, Hasler R, Little RD, Huse K, Ruether A,
668 Balschun T et al. 2007. Systematic association mapping identifies NELL1 as a novel IBD
669 disease gene. *PLoS One* **2**: e691.

670 Frochot V, Alqub M, Cattin AL, Carriere V, Houllier A, Baraille F, Barbot L, Saint-Just S, Ribeiro
671 A, Lacasa M et al. 2012. The transcription factor HNF-4alpha: a key factor of the intestinal
672 uptake of fatty acids in mouse. *Am J Physiol Gastrointest Liver Physiol* **302**: G1253-1263.

673 Gkouskou KK, Ioannou M, Pavlopoulos GA, Georgila K, Siganou A, Nikolaidis G, Kanellis DC,
674 Moore S, Papadakis KA, Kardassis D et al. 2016. Apolipoprotein A-I inhibits experimental colitis
675 and colitis-propelled carcinogenesis. *Oncogene* **35**: 2496-2505.

676 Haberman Y, Tickle TL, Dexheimer PJ, Kim MO, Tang D, Karns R, Baldassano RN, Noe JD,
677 Rosh J, Markowitz J et al. 2014. Pediatric Crohn disease patients exhibit specific ileal
678 transcriptome and microbiome signature. *J Clin Invest* **124**: 3617-3633.

679 Hertz R, Magenheim J, Berman I, Bar-Tana J. 1998. Fatty acyl-CoA thioesters are ligands of
680 hepatic nuclear factor-4alpha. *Nature* **392**: 512-516.

681 Hong YH, Varanasi US, Yang W, Leff T. 2003. AMP-activated protein kinase regulates
682 HNF4alpha transcriptional activity by inhibiting dimer formation and decreasing protein stability.
683 *J Biol Chem* **278**: 27495-27501.

684 Hrabovsky V, Zadak Z, Blaha V, Hyspler R, Karlik T, Martinek A, Mendlova A. 2009. Cholesterol
685 metabolism in active Crohn's disease. *Wien Klin Wochenschr* **121**: 270-275.

686 Huang J, Levitsky LL, Rhoads DB. 2009. Novel P2 promoter-derived HNF4alpha isoforms with
687 different N-terminus generated by alternate exon insertion. *Exp Cell Res* **315**: 1200-1211.

688 Jager S, Handschin C, St-Pierre J, Spiegelman BM. 2007. AMP-activated protein kinase
689 (AMPK) action in skeletal muscle via direct phosphorylation of PGC-1alpha. *Proc Natl Acad Sci*
690 *U S A* **104**: 12017-12022.

691 Jostins L Ripke S Weersma RK Duerr RH McGovern DP Hui KY Lee JC Schumm LP Sharma Y
692 Anderson CA et al. 2012. Host-microbe interactions have shaped the genetic architecture of
693 inflammatory bowel disease. *Nature* **491**: 119-124.

694 Kamada N, Seo SU, Chen GY, Nunez G. 2013. Role of the gut microbiota in immunity and
695 inflammatory disease. *Nat Rev Immunol* **13**: 321-335.

696 Kanther M, Sun X, Muhlbauer M, Mackey LC, Flynn EJ, 3rd, Bagnat M, Jobin C, Rawls JF.
697 2011. Microbial colonization induces dynamic temporal and spatial patterns of NF-kappaB
698 activation in the zebrafish digestive tract. *Gastroenterology* **141**: 197-207.

699 Klapper M, Bohme M, Nitz I, Doring F. 2007. The human intestinal fatty acid binding protein
700 (hFABP2) gene is regulated by HNF-4alpha. *Biochem Biophys Res Commun* **356**: 147-152.

701 Korecka A, de Wouters T, Cultrone A, Lapaque N, Pettersson S, Dore J, Blottiere HM,
702 Arulampalam V. 2013. ANGPTL4 expression induced by butyrate and rosiglitazone in human
703 intestinal epithelial cells utilizes independent pathways. *Am J Physiol Gastrointest Liver Physiol*
704 **304**: G1025-1037.

705 Krautkramer KA, Kreznar JH, Romano KA, Vivas EI, Barrett-Wilt GA, Rabaglia ME, Keller MP,
706 Attie AD, Rey FE, Denu JM. 2016. Diet-Microbiota Interactions Mediate Global Epigenetic
707 Programming in Multiple Host Tissues. *Mol Cell* **64**: 982-992.

708 Li Y, Rao X, Mattox WW, Amos CI, Liu B. 2015. RNA-Seq Analysis of Differential Splice
709 Junction Usage and Intron Retentions by DEXSeq. *PLoS One* **10**: e0136653.

Love MI, Huber W, Anders S. 2014. Moderated estimation of fold change and dispersion for RNA-seq data with DESeq2. *Genome Biol* **15**: 550.

Ma R, Yang H, Li J, Yang X, Chen X, Hu Y, Wang Z, Xue L, Zhou W. 2016. Association of HNF4alpha gene polymorphisms with susceptibility to type 2 diabetes. *Mol Med Rep* **13**: 2241-2246.

Marcil V, Seidman E, Sinnett D, Boudreau F, Gendron FP, Beaulieu JF, Menard D, Precourt LP, Amre D, Levy E. 2010. Modification in oxidative stress, inflammation, and lipoprotein assembly in response to hepatocyte nuclear factor 4alpha knockdown in intestinal epithelial cells. *J Biol Chem* **285**: 40448-40460.

Marcil V, Sinnett D, Seidman E, Boudreau F, Gendron FP, Beaulieu JF, Menard D, Lambert M, Bitton A, Sanchez R et al. 2012. Association between genetic variants in the HNF4A gene and childhood-onset Crohn's disease. *Genes Immun* **13**: 556-565.

Marjoram L, Alvers A, Deerhake ME, Bagwell J, Mankiewicz J, Cocchiaro JL, Beerman RW, Willer J, Sumigray KD, Katsanis N et al. 2015. Epigenetic control of intestinal barrier function and inflammation in zebrafish. *Proc Natl Acad Sci U S A* **112**: 2770-2775.

Mbodji K, Charpentier C, Guerin C, Querec C, Bole-Feysot C, Aziz M, Savoye G, Dechelotte P, Marion-Letellier R. 2013. Adjunct therapy of n-3 fatty acids to 5-ASA ameliorates inflammatory score and decreases NF-kappaB in rats with TNBS-induced colitis. *J Nutr Biochem* **24**: 700-705.

Meddens CA, Harakalova M, van den Dungen NA, Foroughi Asl H, Hijma HJ, Cuppen EP, Bjorkegren JL, Asselbergs FW, Nieuwenhuis EE, Mokry M. 2016. Systematic analysis of chromatin interactions at disease associated loci links novel candidate genes to inflammatory bowel disease. *Genome Biol* **17**: 247.

Mokry M, Middendorp S, Wiegerinck CL, Witte M, Teunissen H, Meddens CA, Cuppen E, Clevers H, Nieuwenhuis EE. 2014. Many inflammatory bowel disease risk loci include regions that regulate gene expression in immune cells and the intestinal epithelium. *Gastroenterology* **146**: 1040-1047.

Morgun A, Dzutsev A, Dong X, Greer RL, Sexton DJ, Ravel J, Schuster M, Hsiao W, Matzinger P, Shulzhenko N. 2015. Uncovering effects of antibiotics on the host and microbiota using transkingdom gene networks. *Gut* **64**: 1732-1743.

Nijmeijer RM, Gadaleta RM, van Mil SW, van Bodegraven AA, Crusius JB, Dijkstra G, Hommes DW, de Jong DJ, Stokkers PC, Verspaget HW et al. 2011. Farnesoid X receptor (FXR) activation and FXR genetic variation in inflammatory bowel disease. *PLoS One* **6**: e23745.

O'Shea EF, Cotter PD, Stanton C, Ross RP, Hill C. 2012. Production of bioactive substances by intestinal bacteria as a basis for explaining probiotic mechanisms: bacteriocins and conjugated linoleic acid. *Int J Food Microbiol* **152**: 189-205.

Palanker L, Tennessen JM, Lam G, Thummel CS. 2009. Drosophila HNF4 regulates lipid mobilization and beta-oxidation. *Cell Metab* **9**: 228-239.

Plevy S, Silverberg MS, Lockton S, Stockfisch T, Croner L, Stachelski J, Brown M, Triggs C, Chuang E, Princen F et al. 2013. Combined serological, genetic, and inflammatory markers

differentiate non-IBD, Crohn's disease, and ulcerative colitis patients. *Inflamm Bowel Dis* **19**: 1139-1148.

Qin J, Li Y, Cai Z, Li S, Zhu J, Zhang F, Liang S, Zhang W, Guan Y, Shen D et al. 2012. A metagenome-wide association study of gut microbiota in type 2 diabetes. *Nature* **490**: 55-60.

Rabot S, Membrez M, Bruneau A, Gerard P, Harach T, Moser M, Raymond F, Mansourian R, Chou CJ. 2010. Germ-free C57BL/6J mice are resistant to high-fat-diet-induced insulin resistance and have altered cholesterol metabolism. *FASEB J* **24**: 4948-4959.

Rawls JF, Samuel BS, Gordon JI. 2004. Gnotobiotic zebrafish reveal evolutionarily conserved responses to the gut microbiota. *Proc Natl Acad Sci U S A* **101**: 4596-4601.

Rha GB, Wu G, Shoelson SE, Chi YI. 2009. Multiple binding modes between HNF4alpha and the LXXLL motifs of PGC-1alpha lead to full activation. *J Biol Chem* **284**: 35165-35176.

San Roman AK, Aronson BE, Krasinski SD, Shivdasani RA, Verzi MP. 2015. Transcription factors GATA4 and HNF4A control distinct aspects of intestinal homeostasis in conjunction with transcription factor CDX2. *J Biol Chem* **290**: 1850-1860.

Sartor RB, Wu GD. 2016. Roles for Intestinal Bacteria, Viruses, and Fungi in Pathogenesis of Inflammatory Bowel Diseases and Therapeutic Approaches. *Gastroenterology* doi:10.1053/j.gastro.2016.10.012.

Semenkovich NP, Planer JD, Ahern PP, Griffin NW, Lin CY, Gordon JI. 2016. Impact of the gut microbiota on enhancer accessibility in gut intraepithelial lymphocytes. *Proc Natl Acad Sci U S A* doi:10.1073/pnas.1617793113.

Semova I, Carten JD, Stombaugh J, Mackey LC, Knight R, Farber SA, Rawls JF. 2012. Microbiota regulate intestinal absorption and metabolism of fatty acids in the zebrafish. *Cell Host Microbe* **12**: 277-288.

Shulzhenko N, Morgun A, Hsiao W, Battle M, Yao M, Gavrilova O, Orandle M, Mayer L, Macpherson AJ, McCoy KD et al. 2011. Crosstalk between B lymphocytes, microbiota and the intestinal epithelium governs immunity versus metabolism in the gut. *Nat Med* **17**: 1585-1593.

Soutoglou E, Katrakili N, Talianidis I. 2000. Acetylation regulates transcription factor activity at multiple levels. *Mol Cell* **5**: 745-751.

Staiger H, Haas C, Machann J, Werner R, Weisser M, Schick F, Machicao F, Stefan N, Fritsche A, Haring HU. 2009. Muscle-derived angiopoietin-like protein 4 is induced by fatty acids via peroxisome proliferator-activated receptor (PPAR)-delta and is of metabolic relevance in humans. *Diabetes* **58**: 579-589.

Stegmann A, Hansen M, Wang Y, Larsen JB, Lund LR, Ritie L, Nicholson JK, Quistorff B, Simon-Assmann P, Troelsen JT et al. 2006. Metabolome, transcriptome, and bioinformatic cis-element analyses point to HNF-4 as a central regulator of gene expression during enterocyte differentiation. *Physiol Genomics* **27**: 141-155.

785 Thaiss Christoph A, Levy M, Korem T, Dohnalová L, Shapiro H, Jaitin Diego A, David E, Winter
786 Deborah R, Gury-BenAri M, Tatirovsky E et al. 2016. Microbiota Diurnal Rhythmicity Programs
787 Host Transcriptome Oscillations. *Cell* **167**: 1495-1510.e1412.

788 Trapnell C, Hendrickson DG, Sauvageau M, Goff L, Rinn JL, Pachter L. 2013. Differential
789 analysis of gene regulation at transcript resolution with RNA-seq. *Nat Biotech* **31**: 46-53.

790 Tremblay E, Thibault MP, Ferretti E, Babakissa C, Bertelle V, Bettolli M, Burghardt KM,
791 Colombani JF, Grynspan D, Levy E et al. 2016. Gene expression profiling in necrotizing
792 enterocolitis reveals pathways common to those reported in Crohn's disease. *BMC Med*
793 *Genomics* **9**: 6.

794 Veilleux A, Mayeur S, Berube JC, Beaulieu JF, Tremblay E, Hould FS, Bosse Y, Richard D,
795 Levy E. 2015. Altered intestinal functions and increased local inflammation in insulin-resistant
796 obese subjects: a gene-expression profile analysis. *BMC Gastroenterol* **15**: 119.

797 Vrieze A, Van Nood E, Holleman F, Salojarvi J, Kootte RS, Bartelsman JF, Dallinga-Thie GM,
798 Ackermans MT, Serlie MJ, Oozeer R et al. 2012. Transfer of intestinal microbiota from lean
799 donors increases insulin sensitivity in individuals with metabolic syndrome. *Gastroenterology*
800 **143**: 913-916.e917.

801 Weissglas-Volkov D, Huertas-Vazquez A, Suviolahti E, Lee J, Plaisier C, Canizales-Quinteros
802 S, Tusie-Luna T, Aguilar-Salinas C, Taskinen MR, Pajukanta P. 2006. Common hepatic nuclear
803 factor-4alpha variants are associated with high serum lipid levels and the metabolic syndrome.
804 *Diabetes* **55**: 1970-1977.

805 Yuan X, Ta TC, Lin M, Evans JR, Dong Y, Bolotin E, Sherman MA, Forman BM, Sladek FM.
806 2009. Identification of an endogenous ligand bound to a native orphan nuclear receptor. *PLoS*
807 *One* **4**: e5609.

808 Zhang Y, Liu T, Meyer CA, Eeckhoute J, Johnson DS, Bernstein BE, Nusbaum C, Myers RM,
809 Brown M, Li W et al. 2008. Model-based analysis of ChIP-Seq (MACS). *Genome Biol* **9**: R137.

810

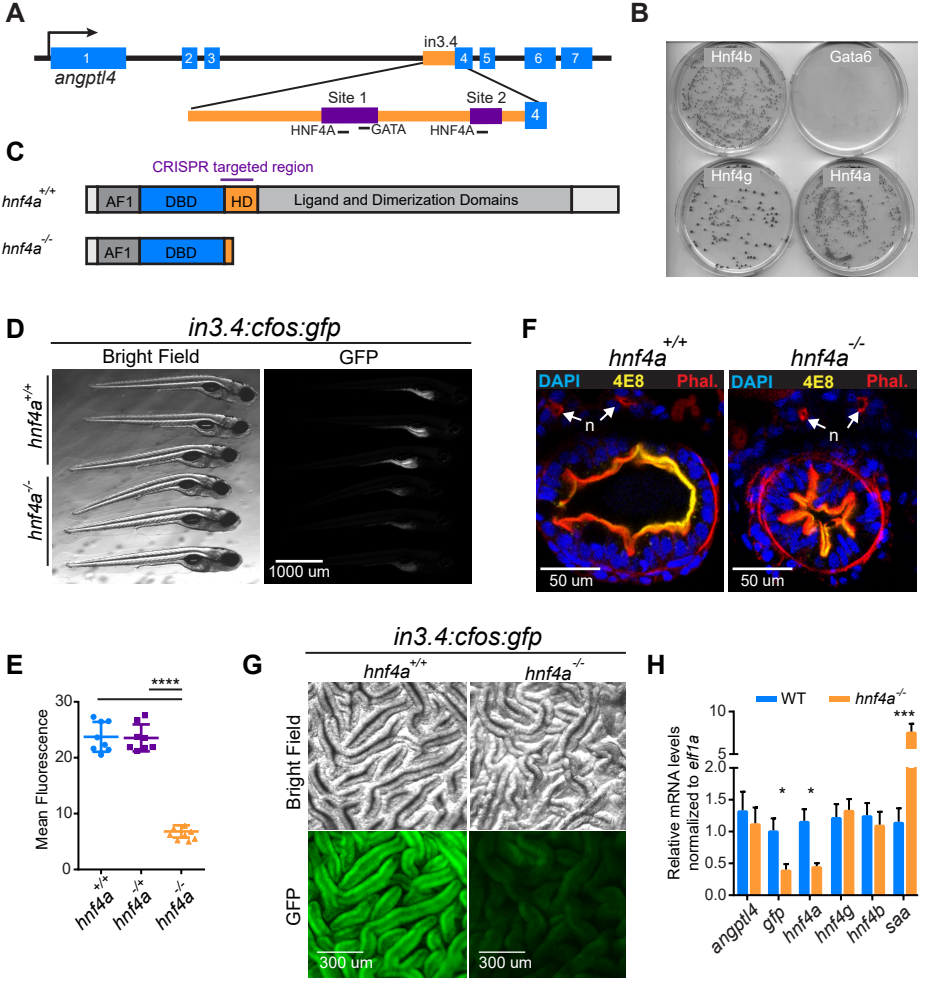
A
1
2
3
in3.4
4
5
6
7
angptl4
Site 1
Site 2
4
HNF4A
GATA
HNF4A
B
Hnf4b
Gata6
Hnf4g
Hnf4a
C
CRISPR targeted region
hnf4a+/+
AF1
DBD
HD
Ligand and Dimerization Domains
hnf4a-/-
AF1
DBD
D
in3.4:cfos:gfp
Bright Field
GFP
hnf4a+/+
hnf4a-/-
1000 um
F
hnf4a+/+
hnf4a-/-
DAPI
4E8
Phal.
n
50 um
E
****
Mean Fluorescence
30
20
10
0
+/+
-/+
-/-
hnf4a
G
in3.4:cfos:gfp
hnf4a+/+
hnf4a-/-
Bright Field
GFP
300 um
H
WT
hnf4a-/-
***
*
*
Relative mRNA levels normalized to elf1a
10
5
2.0
1.5
1.0
0.5
0.0
angptl4
gfp
hnf4a
hnf4g
hnf4b
saa

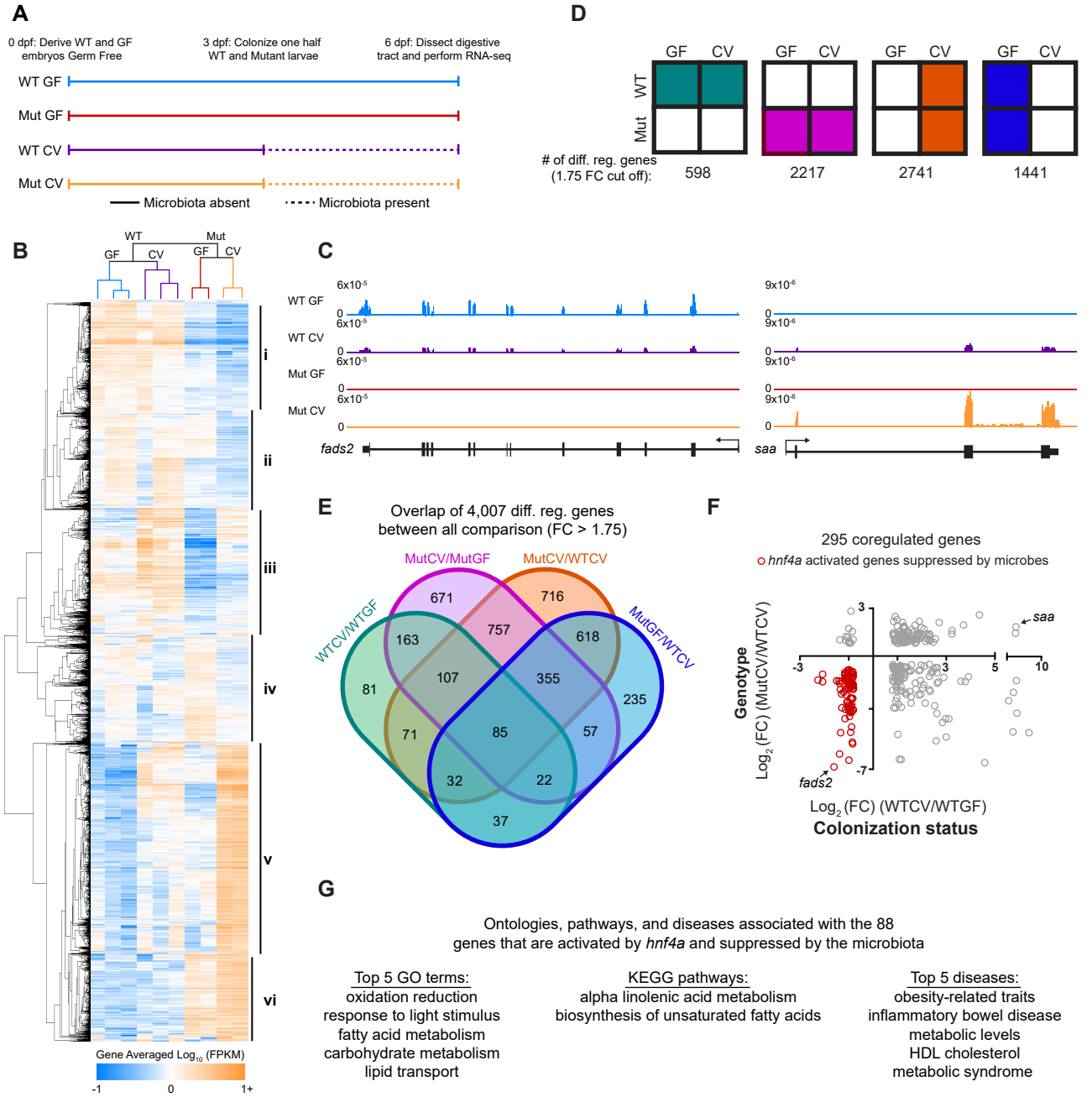
A
0 dpf: Derive WT and GF embryos Germ Free
3 dpf: Colonize one half WT and Mutant larvae
6 dpf: Dissect digestive tract and perform RNA-seq
WT GF
Mut GF
WT CV
Mut CV
Microbiota absent
Microbiota present
D
GF CV GF CV GF CV GF CV
WT
Mut
# of diff. reg. genes (1.75 FC cut off):
598
2217
2741
1441
B
WT Mut
GF CV GF CV
i
ii
iii
iv
v
vi
Gene Averaged Log10 (FPKM)
-1 0 1+
C
WT GF
WT CV
Mut GF
Mut CV
6x10-5
9x10-6
fads2
saa
E
Overlap of 4,007 diff. reg. genes between all comparison (FC > 1.75)
MutCV/MutGF
MutCV/WTCV
WTCV/WTGF
MutGF/WTCV
671
716
757
163
618
107
355
81
235
71
85
57
32
22
37
F
295 coregulated genes
hnf4a activated genes suppressed by microbes
Genotype
Log2 (FC) (MutCV/WTCV)
Log2 (FC) (WTCV/WTGF)
Colonization status
saa
fads2
G
Ontologies, pathways, and diseases associated with the 88 genes that are activated by hnf4a and suppressed by the microbiota
Top 5 GO terms:
oxidation reduction
response to light stimulus
fatty acid metabolism
carbohydrate metabolism
lipid transport
KEGG pathways:
alpha linolenic acid metabolism
biosynthesis of unsaturated fatty acids
Top 5 diseases:
obesity-related traits
inflammatory bowel disease
metabolic levels
HDL cholesterol
metabolic syndrome

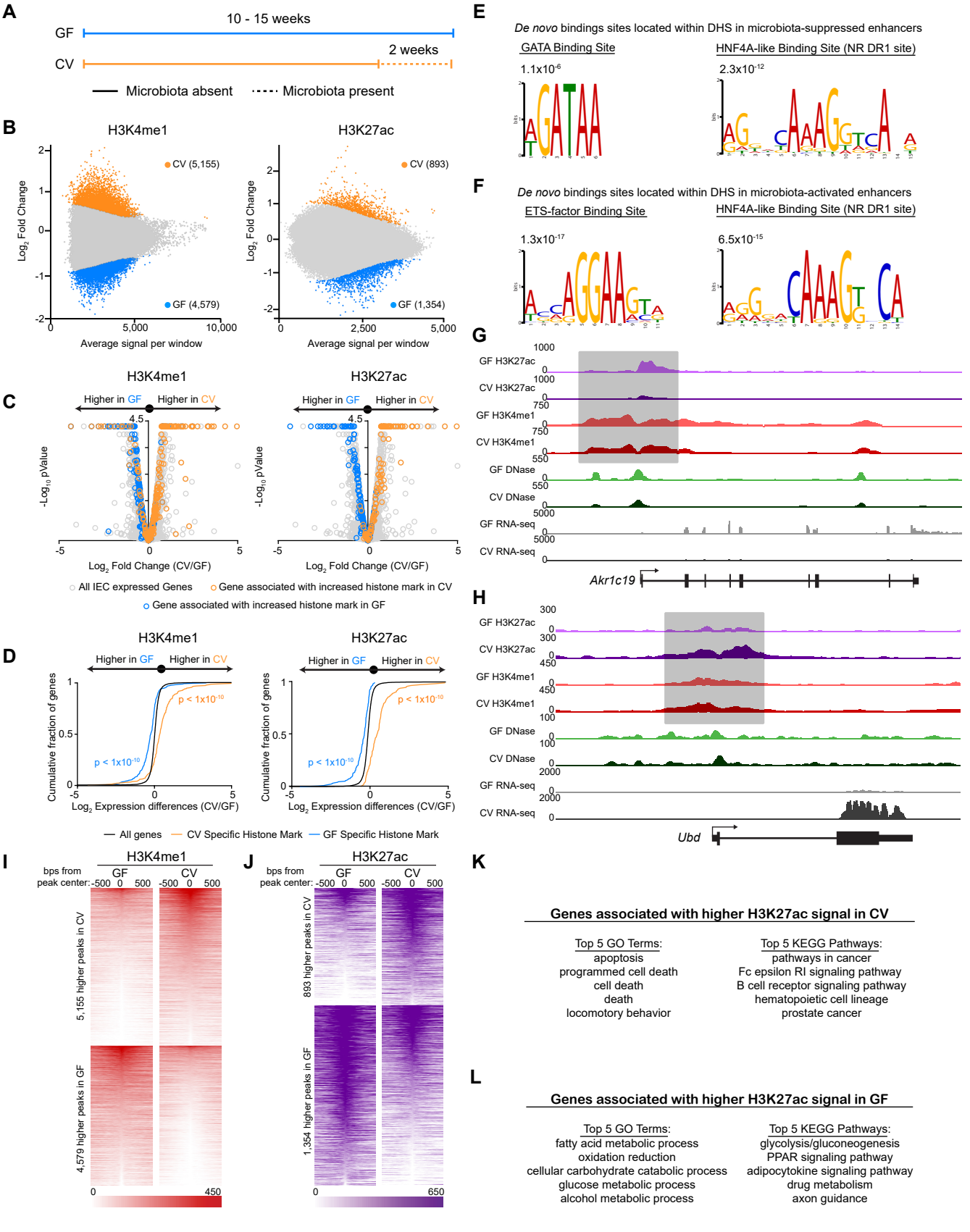
A
10 - 15 weeks
GF
2 weeks
CV
Microbiota absent
Microbiota present
B
H3K4me1
H3K27ac
CV (5,155)
GF (4,579)
CV (893)
GF (1,354)
Log2 Fold Change
Average signal per window
C
H3K4me1
H3K27ac
Higher in GF
Higher in CV
-Log10 pValue
Log2 Fold Change (CV/GF)
All IEC expressed Genes
Gene associated with increased histone mark in CV
Gene associated with increased histone mark in GF
D
H3K4me1
H3K27ac
Cumulative fraction of genes
p < 1x10-10
Log2 Expression differences (CV/GF)
All genes
CV Specific Histone Mark
GF Specific Histone Mark
E
De novo bindings sites located within DHS in microbiota-suppressed enhancers
GATA Binding Site
1.1x10-6
HNF4A-like Binding Site (NR DR1 site)
2.3x10-12
F
De novo bindings sites located within DHS in microbiota-activated enhancers
ETS-factor Binding Site
1.3x10-17
HNF4A-like Binding Site (NR DR1 site)
6.5x10-15
G
GF H3K27ac
CV H3K27ac
GF H3K4me1
CV H3K4me1
GF DNase
CV DNase
GF RNA-seq
CV RNA-seq
Akr1c19
H
GF H3K27ac
CV H3K27ac
GF H3K4me1
CV H3K4me1
GF DNase
CV DNase
GF RNA-seq
CV RNA-seq
Ubd
I
H3K4me1
bps from peak center:
GF
CV
5,155 higher peaks in CV
4,579 higher peaks in GF
J
H3K27ac
893 higher peaks in CV
1,354 higher peaks in GF
K
Genes associated with higher H3K27ac signal in CV
Top 5 GO Terms:
apoptosis
programmed cell death
cell death
death
locomotory behavior
Top 5 KEGG Pathways:
pathways in cancer
Fc epsilon RI signaling pathway
B cell receptor signaling pathway
hematopoietic cell lineage
prostate cancer
L
Genes associated with higher H3K27ac signal in GF
Top 5 GO Terms:
fatty acid metabolic process
oxidation reduction
cellular carbohydrate catabolic process
glucose metabolic process
alcohol metabolic process
Top 5 KEGG Pathways:
glycolysis/gluconeogenesis
PPAR signaling pathway
adipocytokine signaling pathway
drug metabolism
axon guidance

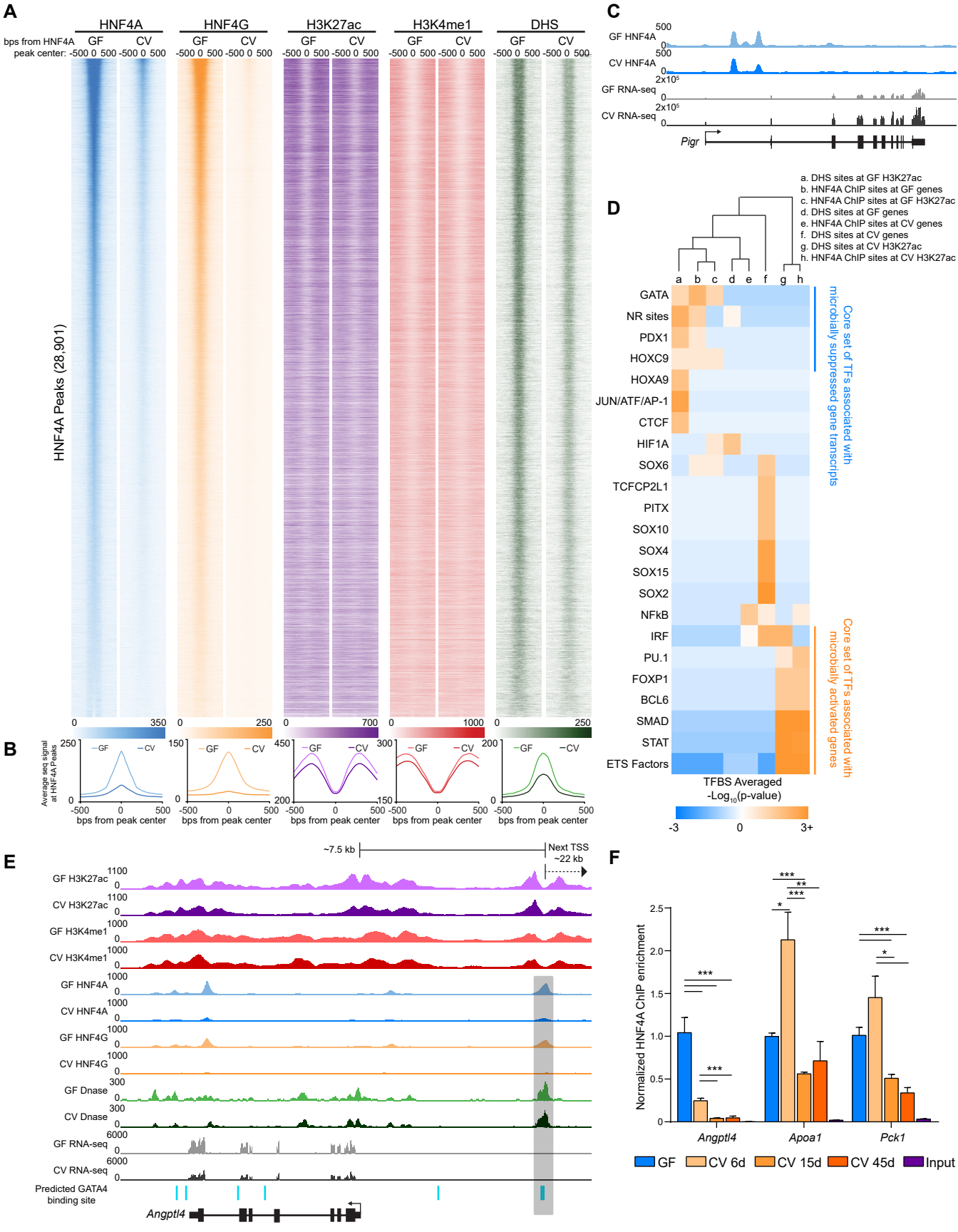
A
HNF4A
HNF4G
H3K27ac
H3K4me1
DHS
GF
CV
bps from HNF4A peak center: -500 0 500
HNF4A Peaks (28,901)
0 350
0 250
0 700
0 1000
0 250
B
Average seq signal at HNF4A Peaks
bps from peak center
C
GF HNF4A
CV HNF4A
GF RNA-seq
CV RNA-seq
Pigr
D
a. DHS sites at GF H3K27ac
b. HNF4A ChIP sites at GF genes
c. HNF4A ChIP sites at GF H3K27ac
d. DHS sites at GF genes
e. HNF4A ChIP sites at CV genes
f. DHS sites at CV genes
g. DHS sites at CV H3K27ac
h. HNF4A ChIP sites at CV H3K27ac
GATA
NR sites
PDX1
HOXC9
HOXA9
JUN/ATF/AP-1
CTCF
HIF1A
SOX6
TCFCP2L1
PITX
SOX10
SOX4
SOX15
SOX2
NFkB
IRF
PU.1
FOXP1
BCL6
SMAD
STAT
ETS Factors
Core set of TFs associated with microbially suppressed gene transcripts
Core set of TFs associated with microbially activated genes
TFBS Averaged -Log10(p-value)
E
~7.5 kb
Next TSS ~22 kb
GF H3K27ac
CV H3K27ac
GF H3K4me1
CV H3K4me1
GF HNF4A
CV HNF4A
GF HNF4G
CV HNF4G
GF Dnase
CV Dnase
GF RNA-seq
CV RNA-seq
Predicted GATA4 binding site
Angptl4
F
Normalized HNF4A ChIP enrichment
Angptl4
Apoa1
Pck1
GF
CV 6d
CV 15d
CV 45d
Input

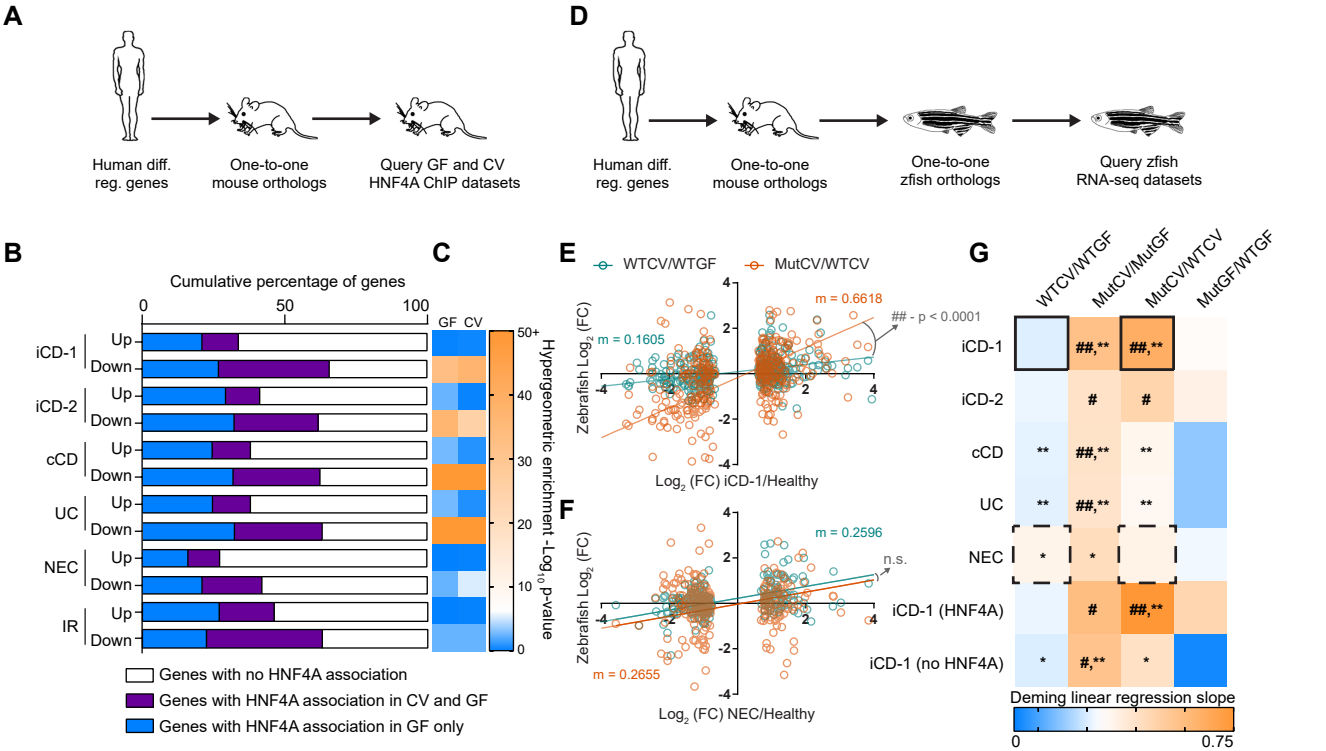

H

iCD DOWN genes with HNF4A ChIP association in mice

Top 5 GO Terms:	Top 5 KEGG Pathways:
cholesterol homeostasis	fat digestion and absorption
transport	protein digestion and absorption
transmembrane transport	vitamin digestion and absorption
sodium ion transport	metabolic process
cholesterol efflux	carbohydrate digestion and aborption

I

iCD UP genes with HNF4A ChIP association in mice

Top 5 GO Terms:	Top 5 KEGG Pathways:
reponse to lipopolysaccharide (lps)	TNF signaling pathway
cellular response to lps	cytokine-cytokine receptor interaction
positive regulation of cell migration	tuberculosis
immune system process	Jak-STAT signaling pathway
response to hypoxia	nitrogen metabolism

J

iCD DOWN genes that lose HNF4A-ChIP association in CV mice

Top 5 GO Terms:	Top 5 KEGG Pathways:
response to toxic substance	fat digestion and absorption
transmembrane transport	histidine metabolism
long-chain fatty acid transport	metabolic process
midgut development	drug metabolism - cytochrome P450
response to drug	phenylalanine metabolism

K

iCD UP genes that lose HNF4A ChIP association in CV mice

Top 5 GO Terms:	Top 5 KEGG Pathways:
reponse to lipopolysaccharide (lps)	cytokine-cytokine receptor interaction
immune response	Jak-STAT signaling pathway
response to hypoxia	nitrogen metabolism
cellular response to lps	TNF signaling pathway
defense response to virus	prolactin signaling pathway